

Proton-Transfer Mechanism in 2-Thioxoimidazolidin-4-one: A Competition between Keto/Enol and Thione/Thiol Tautomerism Reactions

Setodeh Bagheri and Hossein Roohi*

Department of Chemistry, Faculty of Science, University of Sistan and Baluchestan, P.O. Box 98135-674, Zahedan, Iran

Received July 15, 2008; E-mail: hroohi@hamoon.usb.ac.ir

The proton transfer in 2-thioxoimidazolidin-4-one (1,3-IM) via two keto/enol and thione/thiol intramolecular mechanisms was investigated by using DFT (B3LYP) and ab initio (MP2) methods in the gas phase. A conspicuous consistency was found between results of B3LYP and MP2 calculations. The change in structural parameters for direct keto/enol tautomerization is greater than thione/thiol transformation on going from ground state to transition state. At both level of calculations, the computed energy barrier for direct and water-assisted keto/enol tautomerization is higher than the corresponding thione/thiol. The energy barriers for direct proton-transfer tautomerization reactions are significantly greater than H_2O-assisted tautomerization. The NBO results show that the change of electronic charge of hydrogens involved in migration in direct proton transfer is much greater than in the water-assisted mechanism.

The prototropic tautomerism in heterocyclic compounds is relevant in many areas of chemistry and biochemistry. Particularly importants are the oxo/hydroxy and thiol/thione equilibrium.[1–5] The thione/thiol tautomeric equilibrium is the subject of many experimental and theoretical studies.[6–17] A detailed study of the structure and changes in geometric and energetic parameters caused by the migration of hydrogen atom would enable the understanding of the different properties of tautomers. Knowledge of the relative stabilities of tautomeric forms of heterocycles as well as the conversion from one tautomer to another is important from the point of view of structural chemistry.

Since imidazolidine-2,4-dione ring was discovered by Bayer in 1861,[18] a large set of imidazolidine derivatives have been synthesized showing a wide range of biological activities.[19–21] Derivatives of imidazolidine are major drugs currently used for the treatment of hyperthyroidism.[22] These drugs possess a thiourea group which is known to form very stable electron donor–acceptor complexes with the Lewis acid diiodine. These compounds can exhibit thione/thiol tautomerism. It has been proposed that both thione and thiol tautomers of imidazolidine derivatives are involved in complex formation.[23]

In this work, we have investigated proton transfer via intramolecular and water-assisted mechanisms in 2-thioxoimidazolidin-4-one (1,3-IM) by using DFT (B3LYP) and ab initio (MP2) methods. This compound exhibits both keto/enol and thione/thiol equilibriums. In fact, a competition on the proton transfer in these two processes is predicted. This allowed us to compare different tautomerism reaction processes. Hence, energy barriers for proton transfer via intramolecular and water-assisted mechanisms are also evaluated. The origin of preference is analyzed by natural bond orbital (NBO) method.

Computational Details

All calculations were performed using Gaussian 98[24] program package. The geometries of the reactants and products for the tautomerization of the isolated compound were optimized using MP2 and B3LYP methods applying 6-31++G(2d,2p) basis sets. DFT offers an electron correlation correction frequently comparable to the MP2 or in certain cases, and for certain purposes even superior to MP2, but at considerably lower computational cost.[25] Vibrational frequencies have been obtained at the same levels for characterization of stationary points and calculation of thermal and zero-point energy corrections. Natural bond orbital (NBO)[26] analysis was carried out with version 3.1 included in Gaussian 98 program at MP2/6-31++G(2d,2p) level of theory.

Results and Discussion

Direct Proton-Transfer Mechanism. The equilibrium structures for different paths of direct proton transfer are depicted in Figure 1. The structural parameters calculated at MP2/6-31++G(2d,2p) level of theory are listed in Table 1. Transition-state structures (TSs) were confirmed to be the first-order saddle point on the tautomerization pathway. The C2–N3 distance involved in thione/thiol tautomerization is influenced by the presence of CO groups. As can be seen in Table 1, the C2–N3 bond distance in 1,3-IM is greater than C2–N1, because the presence of a CO group in the vicinity of N3 atom reduces charge transfer from N3 to CS.

Tautomeric interconversion in 1,3-IM may occurs via four paths: (1,3-IM → TS1 → $1,2_S$-IM), (1,3-IM → TS2 → $1,4_O$-IM), (1,3-IM → TS3 → 2_S,3-IM), and (1,3-IM → TS4 → $1,3\text{-}4_O$-IM). These paths are labeled as P1, P2, P3, and P4, respectively. Thione/thiol tautomerization is performed in the first and third paths while keto/enol tautomerization is carried out in the second and fourth paths. For proton-transfer mechanisms, comparison of geometries shows that the structural parameters in stationary points change upon tautomerization. In particular, C–NH bond lengths in P1, P2, and P3 paths

Published on the web April 11, 2009; doi:10.1246/bcsj.82.446

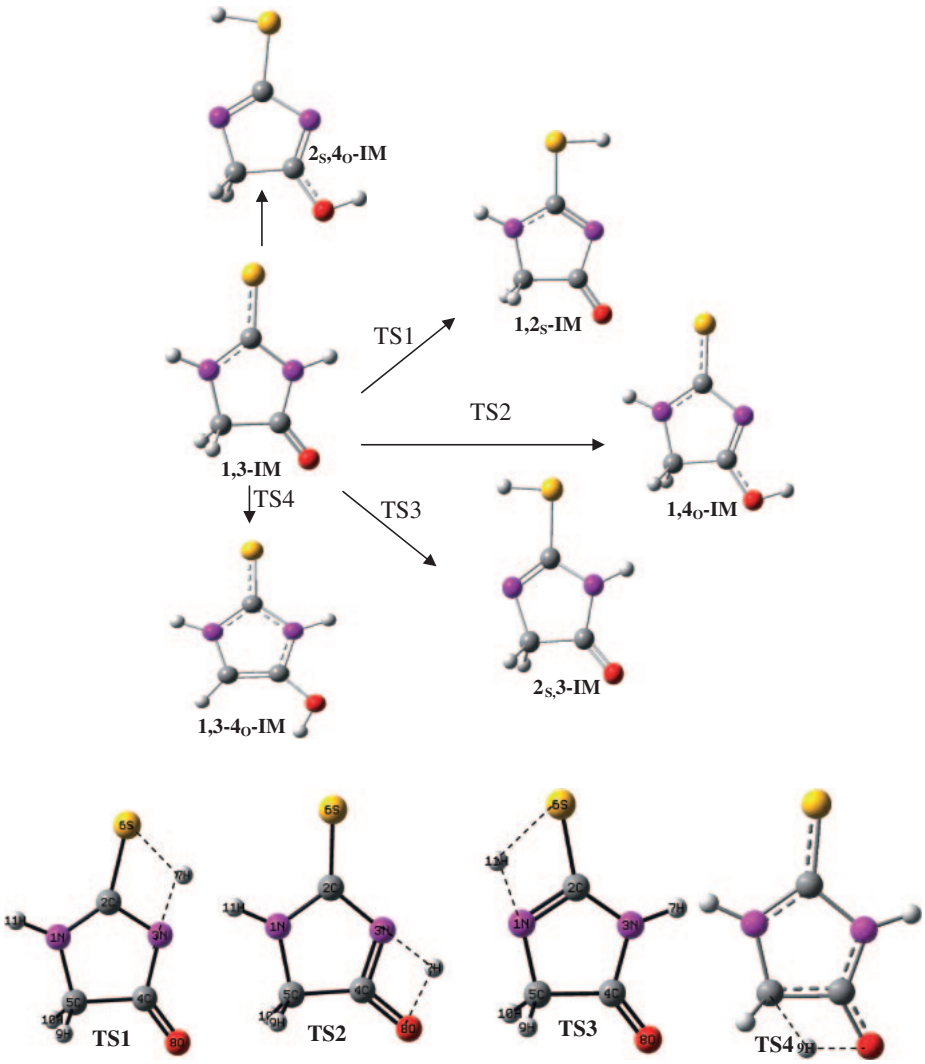

Figure 1. The paths of proton transfer in 2-thioxoimidazolidin-4-one.

and C5–CO in the P4 path reduce, while the C=S(O) distances increase in going from 1,3-IM to TSs. The N–H and C5–H bonds are lengthened and NCS(O) and C5C4O bond angles are also compressed because of intramolecular hydrogen bonding. The N–H distance is 1.008 Å in 1,3-IM, 1.385(1.371) Å in TS1(TS3), and 1.344 Å in TS2. These structural changes reveal that the N–H bond is nearly broken and the S(O)–H bond is almost formed in TSs and an H atom is transferring from the N atom to the S(O) atoms. The C5–H9 bond length also increases on going from 1,3-IM to TS4 by 0.44 Å. It is clear that the S···H and O···H distances play an important role in the intramolecular proton-transfer reaction. The change of S···H7(H11) distance in going from 1,3-IM to TS1(TS3) is 1.265(1.214) Å and that of O···H7 and O···H9 distances is 1.315 and 1.477 Å in going from 1,3-IM to TS2 and TS4, respectively. The change in C4–N3 and C4–O bond lengths involved in keto/enol tautomerization is greater than those of C2–N and C2–S that participate in thione/thiol tautomerization. In addition, S···H···N and O···H···N angles are 109.3(108.3°) and 103.5° in TS1(TS3) and TS2, respectively. Thus, linearity of the S···H···N angle is greater than the O···H···N. As a result, change in structural parameters in going from 1,3-IM to TS2 (P1 path) and TS4 (P4 path) is bigger than those of P1 and P3 which lead to a very high barrier for P2 and P4 paths (see Table 3). The change in structural parameters in the P4 path is even greater than P2. Therefore, it is expected that the energy barrier for P4 be bigger than other paths.

Table 2 gives the tautomerism energies at various level of theory. B3LYP and MP2 computations suggest predominance of 1,3-IM tautomer over the thiol and enol tautomers. The order of energy of tautomers without considering zero-point vibrational energy (ZPVE) and thermal energy corrections is 1,3-IM < 2_S,3-IM < $1,4_O$-IM < $1,2_S$-IM < 1,3-4_O-IM < 1,3-4_O-IM < $2_S,4_O$-IM. The energy difference between two $1,2_S$-IM and $1,4_O$-IM tautomers is small. Inclusion of ZPVE and thermal energy corrections decrease the energy difference between 1,3-IM and the corresponding tautomers.

In a NBO representation, the diagonal elements of the Fock matrix represent the energies of localized bonds, lone pairs, antibonds, and Rydberg orbitals; off-diagonal elements are bond–antibond, lone pair–antibond, and antibond–antibond interactions, which allow assessment of delocalizations effects. The interaction between filled and vacant orbitals indicates the deviation of the molecule from the Lewis structure and can be

Table 1. The Optimized Geometries (Distances in Å and Angles in °) for Tautomers and TSs Structures Involved in Direct Proton Transfer at MP2/6-31++G(2d,2p) Level[a)]

	IM1	IM2	IM3	IM4	IM5	IM6	TS1	TS2	TS3	TS4
C2–S6	1.750	1.643	1.636	1.76	1.751	1.667	1.702	1.634	1.704	1.645
N1–C2	1.356	1.357	1.369	1.289	1.296	1.365	1.335	1.377	1.317	1.426
C2–N3	1.312	1.394	1.430	1.395	1.427	1.379	1.352	1.412	1.373	1.356
N3–C4	1.412	1.384	1.287	1.394	1.294	1.375	1.401	1.318	1.404	1.346
C4–C5	1.548	1.530	1.502	1.529	1.501	1.365	1.555	1.499	1.541	1.427
C5–N1	1.450	1.450	1.443	1.471	1.464	1.398	1.458	1.458	1.466	1.437
C5–H9	1.089	1.091	1.093	1.090	1.092	2.624	1.090	1.092	1.090	1.529
C5–H10	1.089	1.091	1.093	1.090	1.092	1.074	1.090	1.092	1.090	1.087
C4–O8	1.212	1.213	1.335	1.214	1.336	1.356	1.211	1.278	1.210	1.288
N1–H11	1.005	1.006	1.006			1.006	1.005	1.006	1.371	1.010
S6–H7	1.338	2.933					1.668			
N3–H7		1.008		1.008		1.007	1.385	1.344	1.008	1.007
O8–H7(H9)		2.690 (2.820)[b)]	0.969		0.969	0.963[b)]		1.375		1.343[b)]
S6–H11		2.916		1.339	1.339				1.702	
N1–C2–N3	117.0	105.5	108.2	115.8	118.6	103.1	113.9	104.9	113.0	104.9
C2–N3–C4	105.4	113.8	106.2	108.9	101.9	111.5	109.0	110.7	109.6	109.2
N3–C4–C5	108.9	105.0	115.7	103.0	112.9	107.7	105.8	112.1	104.8	110.7
C4–C5–N1	100.7	102.0	97.6	107.0	102.9	105.2	102.5	98.1	103.5	101.8
C5–N1–C2	108.0	113.7	112.3	105.3	103.7	112.4	108.9	114.3	109.1	112.8
N1–C2–S6	119.3	128.4	126.6	126.1	126.1	128.9	137.0	104.9	110.9	130.1
S6–C2–N3	123.7	126.0	125.3	118.1	115.3	127.9	109.1	128.0	136.1	124.9
N3(C5)–C4–O8	126.5	127.4	125.3	126.7	125.3	134.5[c)]	129.2	110.8	126.4	115.3[c)]
H7–S6–C2	92.3						62.4			
H11–N1–C2	125.3	120.3	121.6			121.1	124.5	120.6	79.9	120.2
C2–N3–H7		122.0		127.1		122.5	79.3		126.3	120.4
C4–O8–H7(H9)			106.9		107.2	108.8[d)]		72.9		71.9[d)]

a) IM1 = 1,2$_S$-IM, IM2 = 1,3-IM, IM3 = 1,4$_O$-IM, IM4 = 2$_S$,3-IM, IM5 = 2$_S$,4$_O$-IM, and IM6 = 1,3-4$_O$-IM. b) O8–H9. c) C5–C4–O8. d) C4–O8–H9.

Table 2. Gas-Phase Calculated Dipole Moment and Relative Energy (kJ mol^{-1}) of Tautomers Involved in Direct Proton-Transfer Reactions

	ΔE_{elec}	ΔE_0[a)]	ΔE[b)]	ΔH[c)]	ΔG[d)]	μ
MP2/6-31++G(2d,2p)						
1,3-IM	0.0	0.0	0.0	0.0	0.0	3.4
1,2$_S$-IM	78.4	67.0	54.7	54.7	59.5	6.3
2$_S$,3-IM	61.3	50.6	40.3	40.3	42.5	2.8
1,4$_O$-IM	76.0	75.1	71.6	71.6	79.7	5.4
2$_S$,4$_O$-IM	105.6	96.1	86.1	86.1	90.5	1.8
1,3-4$_O$-IM	80.5	78.4	77.1	77.1	78.6	6.7
B3LYP/6-31++G(2d,2p)						
1,3-IM	0.00	0.00	0.00	0.00	0.00	3.1
1,2$_S$-IM	80.1	68.2	55.8	55.8	57.5	5.8
2$_S$,3-IM	67.3	56.4	46.2	46.2	45.5	2.4
1,4$_O$-IM	77.0	75.9	74.7	74.7	74.7	5.8
2$_S$,4$_O$-IM	114.9	105.3	95.6	95.6	96.9	1.9
1,3-4$_O$-IM	84.3	82.9	82.4	82.4	81.7	6.7

a) $E_0 = E_{elec}$ + ZPE. b) E_0 + thermal energy. c) E_0 + thermal enthalpy. d) E_0 + thermal Gibbs free energy.

used as a measure of delocalization and hyperconjugation. For each donor NBO (i) and acceptor NBO (j), the stabilization energy $E^{(2)}$ associated with delocalization $i \rightarrow j$ is estimated as $E^{(2)} = -q_j F(i,j)^2/(\varepsilon_j - \varepsilon_i)$, where q_j is the donor orbital occupancy, ε_i and ε_j are diagonal elements (energies of i and j NBOs), and $F(i,j)$ is the off-diagonal NBO Fock matrix element.[26]

The second-order perturbation analysis clearly evidences two major intramolecular interactions involving charge transfer from the nitrogen lone pair (lp$_N$) to σ^*_{C-S} and σ^*_{C-O} antibonding orbitals in most stable tautomer 1,3-IM. The $E^{(2)}$ values for $lp_{N3} \rightarrow \sigma^*$(C–S), $lp_{N1} \rightarrow \sigma^*_{C-S}$, and $lp_{N3} \rightarrow \sigma^*_{C-O}$ interactions in 1,3-IM are 319.4, 424.7, and 313.1 kJ mol^{-1}, respectively. Thus, lower energy for 1,3-IM is expected because of these stronger interactions. These interactions are replaced by $lp_{N3} \rightarrow \sigma^*_{C-O}$ (290.0 kJ mol^{-1}) and $lp_{N3} \rightarrow \sigma^*_{N1-C2}$ (254.4 kJ mol^{-1}) in 2$_S$,3-IM, $lp_{N1} \rightarrow \sigma^*_{C-S}$ (380.0 kJ mol^{-1}) in 1,4$_O$-IM, $lp_{N1} \rightarrow \sigma^*_{C2-N3}$ (384.0 kJ mol^{-1}) in 1,2$_S$-IM, and $lp_{N3} \rightarrow \sigma^*_{C4-C5}$ (53.8 kJ mol^{-1}) and lp(N1) $\rightarrow \sigma^*$(C2–N3) (72.8 kJ mol^{-1}) in 2$_S$,4$_O$-IM. From these data, greater stability of 1,3-IM with respect to the others is completely clear.

The activation energies obtained for proton-jumping reaction are given in Table 3. The electronic energy barriers that emerged from our predictions for paths P1, P2, P3, and P4 are 183.5, 242.2, 180.5, and 330.7 kJ mol^{-1} at MP2/6-31++G(2d,2p) level and 185.0, 243.9, 186.5, and 325.8 kJ mol^{-1} at B3LYP/6-31++G(2d,2p) level. According to the

Table 3. Gas-Phase Calculated Energy Barriers ($kJ\,mol^{-1}$) Corresponding to the Direct and Water-Assisted Proton-Transfer Reactions, Tunneling Crossover Temperatures (K), and Dipole Moments (D)

	$\Delta^{\#}E_{elec}$	$\Delta^{\#}E_0$[a)]	$\Delta^{\#}E$[b)]	$\Delta^{\#}H$[c)]	$\Delta^{\#}G$[d)]	T_{tun}	μ[e)]
MP2/6-31++G(2d,2p)							
1,3-IM → TS1	183.5	166.0	148.0	148.0	151.0	380.5	5.1
1,3-IM → TS2	242.2	226.8	208.8	208.8	216.6	461.6	5.1
1,3-IM → TS3	180.5	163.4	145.1	145.1	149.9	387.2	0.6
1,3-IM → TS4	330.7	314.5	296.7	296.7	302.9	521.1	2.2
AW → AW-TS	94.5	78.8	58.8	58.8	69.5	230.2	3.04
BW → BW-TS	95.9	83.9	69.1	69.1	75.6	297.7	3.88
CW → CW-TS	182.7	169.3	149.7	149.7	166.7	390.4	5.66
B3LYP/6-31++G(2d,2p)							
1,3-IM → TS1	185.0	167.7	149.9	149.9	150.8	399.7	4.8
1,3-IM → TS2	243.9	228.5	213.1	229.3	231.2	467.9	4.8
1,3-IM → TS3	186.5	169.1	151.0	151.0	152.8	406.7	0.5
1,3-IM → TS4	325.8	309.4	292.1	292.1	294.9	508.8	2.3
AW → AW-TS	94.3	77.8	57.8	57.8	66.2	229.4	3.29
BW → BW-TS	94.1	80.8	62.8	62.8	73.4	297.6	4.20
CW → CW-TS	175.1	161.1	141.0	141.0	158.0	381.6	5.32

a) $E_0 = E_{elec} + ZPE$. b) E_0 + thermal energy. c) E_0 + thermal enthalpy. d) E_0 + thermal Gibbs free energy. e) For TSs.

results obtained, proton-jump barrier increases in going from thione/thiol to keto/enol tautomerism. The lowest jump rate is predicted for P3 (N1HCS → N1CSH) and the highest for P4 (C5HCO → C5COH). From the results obtained, it is clear that barrier height is nearly identical in P3 and P1 paths. For P1, P2, P3, and P4, inclusion of ZPVE decreases barrier height to 166.0, 226.8, 163.4, and 314.5 $kJ\,mol^{-1}$ at MP2/6-31++G(2d,2p) level and 167.7, 228.5, 169.1, and 309.4 $kJ\,mol^{-1}$ at B3LYP/6-31++G(2d,2p) level, respectively. The activation enthalpy for direct proton transfers P1, P2, P3, and P4 are 148.0, 208.8, 145.1, and 296.7 $kJ\,mol^{-1}$ at MP2/6-31++G(2d,2p) level and 149.9, 213.1, 151.0, and 292.1 $kJ\,mol^{-1}$ at B3LYP/6-31++G(2d,2p) level, respectively. At all levels, the order of activation Gibbs free energy for proton-jumping paths at MP2/6-31++G(2d,2p) level is: P3 (149.9 $kJ\,mol^{-1}$) < P1 (151.0 $kJ\,mol^{-1}$) < P2 (216.6 $kJ\,mol^{-1}$) < P4 (302.9 $kJ\,mol^{-1}$). An analogous order is found at B3LYP/6-31++G(2d,2p) level. So, the energy barrier for keto/enol processes is greater than for thione/thiol processes. In calculation of energy barrier the consistency between the results of MP2 and B3LYP is conspicuous. From comparison of activation Gibbs free energy and activation enthalpy, it becomes apparent that entropy decreases upon proton transfer. This decrease is greater for keto/enol than thione/thiol processes.

Energetic analysis shows that the direct proton transfers P2 and P4 (keto/enol) are more difficult than the P1 and P3 (thione/thiol) processes both thermodynamically and dynamically. This conclusion from energy data are in agreement with greater structural changes predicted for P2 and P4 with respect to the P1 and P3 paths.

The natural charges obtained from NBO analysis are given in Table 4. From Table 4, electronic charge of the S atom involved in the H-bond in 1,3-IM → TS1(TS3) → $1,2_S$-IM (2_S,3-IM) processes decreases from −0.0961e to −0.0319 (−0.05413e) and then 0.0961 (0.0772e). In contrast, electronic charge of the O atom involved in the H-bond in 1,3-IM → TS2(TS4) → $1,4_O$-IM ($1,3\text{-}4_O$-IM) process increases from −0.5372e to −0.6008 (−0.6940e) and then −0.6726e. Thus, it is expected that the barrier to migration in P1 and P3 is smaller than P2 and P4 paths. On the other hand, the H atom involved in proton-transfer gains an electron in P1 and P3 paths and loses an electron in the P2 path.

The imaginary frequencies associated with the transition states of P1, P2, P3, and P4 paths are 1564.2i, 1897.6i, 1591.6i, and 2142.0i at MP2/6-31++G(2d,2p) level and 1643.2i, 1923.5i, 1671.7i, and 2091.5 cm^{-1} at B3LYP/6-31++G(2d,2p) level. Transition-state theory (TST) provides the estimation of tunneling crossover temperature, T_{tun}, whereas below T_{tun} tunneling becomes dominant and above it tunneling becomes negligible. T_{tun} can be found using the Fermann and Auerbach formula:[27]

$$T_{tun} = \frac{hc|\nu^{\#}|\Delta E^{\#}/k_B}{2\pi\Delta E^{\#} - hc|\nu^{\#}|\ln 2} \quad (1)$$

where, $\Delta E^{\#}$ is the electronic barrier height, h is the Planck constant, c is the light speed, ν is the imaginary frequency (cm^{-1}), and k_B is the Boltzmann constant. Calculated T_{tun} values for P1, P2, P3, and P4 paths are 380.5, 461.6, 387.2, and 521.1 K at MP2/6-31++G(2d,2p) level and 399.7, 467.9, 406.7, and 508.8 K at B3LYP/6-31++G(2d,2p) level (Table 3). Thus, it is expected that the proton tunneling for all paths becomes negligible at room temperature.

Water-Assisted Mechanism. The direct proton transfer would take place through a four-member ring transition structure, which contains an almost broken N1–H7 bond whereas the S(O)–H bond is still not formed. Hence, thione and keto forms cannot easily transfer the proton from the N to S and O, because of a long S(O)–H distance. The highly distorted structure would lead to a very high barrier (see Table 3), indicating that the direct proton transfer in 1,3-IM compound is unlikely to occur in the gas phase. It is expected that the energy barrier for direct proton-transfer tautomerization reactions to be significantly greater than H_2O-assisted tautomerization reactions.

To understand the effect of water on the rate of tautomerization, we have investigated the water-assisted tautomerization in 1,3-IM. After formation of the mono-hydrated tautomers of 1,3-IM, the proton-transfer reactions may occur with a water molecule as a bridge between the sulfur (oxygen) atoms and the NH group. The geometric parameters of the dimers and transition states for the tautomeric interconversion within water-assisted processes (1,3-IM-W → W-TS) are given in Figure 2. Dimers AW and BW are stabilized by two nonlinear S(O)···H12–O13 and O7···H–N HBs with bond angels of 88.6(104.8°) and 150.1(147.0°) at MP2/6-31++G(2d,2p) level, respectively. The calculated intermolecular distances of S(O)···H12O13 in AW and BW complexes are 2.449 and 1.998 Å, respectively. The O13···H7N distances were calculated to be 1.900 Å for AW and 2.010 Å for BW complexes. From comparison between N–H and C–S(O) bond lengths in the dimers AW and BW with corresponding monomers, it is obvious that dimerization yields increasing of the N–H and C–S(O) bond lengths. Thus, proton transfer in these complexes

Table 4. NBO Data Calculated at MP2/6-31++G(2d,2p) Level of Theory[a)]

	IM1	IM2	IM3	IM4	IM5	IM6	TS1	TS2
Charge								
N1	−0.6652	−0.6535	−0.6645	−0.4973	−0.6055	−0.5767	−0.6272	−0.6661
C2	0.2706	0.1913	0.1466	0.226	0.321	0.1607	0.241	0.1672
N3	−0.5917	−0.6743	−0.518	−0.6982	−0.6771	−0.603	−0.6745	−0.6274
C4	0.6319	0.6655	0.5727	0.6578	0.7345	0.4416	0.6531	0.5968
C5	−0.3464	−0.3296	−0.3124	−0.3678	−0.3028	−0.194	−0.3344	−0.3051
S6	0.0961	−0.0961	−0.0409	0.0772	0.0968	−0.2334	−0.0319	−0.0401
H7	0.1751	0.4651	0.5278	0.1683	0.5349	0.4675	0.3316	0.4954
O8	−0.525	−0.5372	−0.6726	−0.5458	−0.7406	−0.694	−0.5268	−0.6008
H9	0.2542	0.2566	0.2544	0.4538	0.2492	0.5203	0.2568	0.2633
H10	0.2542	0.2566	0.2544	0.263	0.2492	0.2492	0.2568	0.2633
H11	0.446	0.4556	0.4524	0.263	0.1402	0.4617	0.4555	0.4537
	TS3	TS4	AW	AW-TS	BW	BW-TS	CW	CW-TS
N1	−0.6067	−0.6015	−0.6473	−0.6426	−0.656	−0.6622	−0.646	−0.5918
C2	0.2148	0.1589	0.2217	0.2778	0.1909	0.186	0.1884	0.1709
N3	−0.6743	−0.6215	−0.6793	−0.7008	−0.6683	−0.6655	−0.663	−0.6176
C4	0.6704	0.5727	0.6646	0.6533	0.6667	0.6299	0.6729	0.6077
C5	−0.3432	−0.4172	−0.3304	−0.3424	−0.3239	−0.3098	−0.3352	−0.4505
S6	−0.0541	−0.1034	−0.154	−0.0823	−0.0861	−0.0849	−0.0919	−0.1612
H7	0.3276	0.4677	0.4838	0.521	0.4878	0.5142	0.4649	0.465
O8	−0.5262	−0.6215	−0.5332	−0.54	−0.5787	−0.6599	−0.5719	−0.6915
H9	0.2633	0.4379	0.2564	0.255	0.2567	0.2557	0.2715	0.2631
H10	0.2633	0.2677	0.2569	0.254	0.256	0.2557	0.2715	0.4469
H11	0.4639	0.4603	0.4547	0.4496	0.4547	0.4511	0.4563	0.4564
H12			0.5047	0.3224	0.5102	0.5188	0.5044	0.525
O13			−1.0005	−0.9447	−1.0114	−0.9519	−1.0165	−0.9432
H14			0.5019	0.5199	0.5015	0.5227	0.4948	0.5209
$E^{(2)}$ ($\sigma \rightarrow \sigma^*$)/kJ mol^{-1}								
			AW	AW-TS	BW	BW-TS	CW	CW-TS
lp(S) → σ^*(O13–H12)			43.2					
lp(S) → σ^*(C2–N3)			102.6 (319.4[b)])	333.1				
lp(N3) → σ^*(O13–H7)				398.1		528.1		
lp(O13) → σ^*(S6–H12)				661.4				
lp(O13) → σ^*(N3–H7)			77.0		41.9			
lp(O8) → σ^*(O13–H12)					36.3	691.2	45.9	369.6
lp(O8) → σ^*(C4–N3)					157.9	647.6	161.4	
lp(O13) → σ^*(C5–H9)							0.5	
lp(O13) → σ^*(C5–H10)							0.5	
lp(O8) → σ^*(C4–C5)							125.3	70.2

a) IM1 = 1,2$_S$-IM, IM2 = 1,3-IM, IM3 = 1,4$_O$-IM, IM4 = 2$_S$,3-IM, IM5 = 2$_S$,4$_O$-IM, and IM6 = 1,3–4$_O$-IM. b) For isolated 1,3-IM.

will occur more easily than in the bare 1,3-IM form. The change of N–H and C–S bonds upon complex formation of AW is greater than those of N–H and C–O bonds upon BW formation. Also, dimerization causes the bond lengths of N3–C2 and N3–C4 decrease. The bond angles of N3–C2–S1 and H7–N3–C2 in complexes are similar to those of related monomers. AW and BW complex formation induces a elongation of the O13–H12 bond in water by 0.011 and 0.010 Å, respectively.

As can be seen in Table 5, binding energies including ZPE and thermal correction energies at B3LYP/6-31++G(2d,2p) and MP2/6-31++G(2d,2p) levels of theory lie in the range between −9.5 to −19.0 and −14.9 to −23.9 kJ mol^{-1}, respectively. These results indicate that the CW is the less stable dimer.

W-TSs are transition states predicted in H_2O-assisted tautomerization of 1,3-IM. The TS structures constitute a first-order saddle point whose negative force constant is assisted by the asymmetric stretch of water. During the H_2O-assisted hydrogen-transfer reactions of (AW → AW-TS) and (BW → BW-TS), the hydrogen of the H_2O migrates to the C=S and C=O group, respectively and the hydrogen of the ring NH moves to the oxygen of H_2O. In other words, the water molecule acts simultaneously as a proton acceptor and donor. The elongation of the C–S(O) bonds and reduction of the C–N bond were observed on going from ground states to TSs. The NH···O and S···HO distances in both of them decrease, while N–H7 and O13–H12 distances increase on going from ground

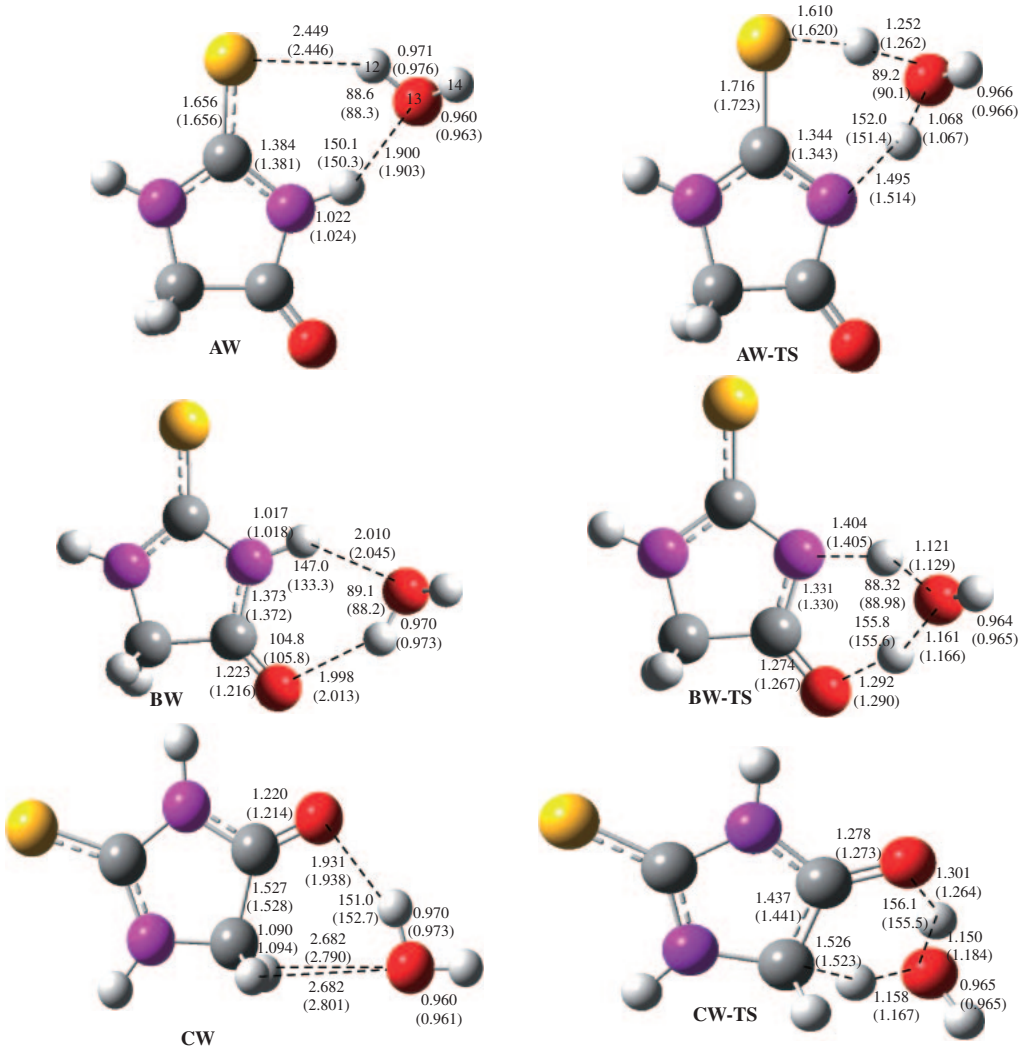

Figure 2. The selected structural parameters of species in water-assisted tautomerization reaction of 2-thioxoimidazolidin-4-one at MP2/6-31++G(2d,2p) and B3LYP/6-31++G(2d,2p) (given in parenthesis) levels of theory.

Table 5. Binding Energies (kJ mol^{-1}) in the H_2O-Assisted Proton-Transfer Mechanisms at B3LYP/6-31++G(2d,2p) and MP2/6-31++G(2d,2p) Levels

	ΔE_{elec}	ΔE_0[a)]	ΔE[b)]	ΔH[c)]	μ
		MP2/6-31++G(2d,2p)			
AW	−41.1	−32.7	−23.9	−26.4	2.83
BW	−38.4	−30.2	−23.6	−26.1	3.62
CW	−31.9	−24.0	−14.9	−17.3	2.29
		B3LYP/6-31++G(2d,2p)			
AW	−36.0	−27.8	−19.0	−21.5	3.00
BW	−32.4	−24.0	−14.8	−17.3	3.78
CW	−26.1	−18.6	−9.5	−12.0	2.14

a) $E_0 = E_{elec}$ + ZPE. b) E_0 + thermal energy. c) E_0 + thermal enthalpy.

states to TSs. The computed N–H···O and S···H–O angles in AW and CW increase on going from ground states to TSs.

In comparison with direct proton transfer, the presence of a water molecule reduces the MP2 calculated Gibbs free energy barrier by 81.5 kJ mol^{-1} in P1 and 141.0 kJ mol^{-1} in P2 path. Thus, tautomerization is facilitated by inclusion of H_2O in both paths. As a result, water-assisted tautomerization is energetically a suitable path for proton transfer. It can be concluded that the direct proton-transition process is more difficult than the water-assisted processes dynamically. In contrast to the gas phase, the difference between the energy barrier for thione–thiol tautomerization in P1 and keto–enol tautomerization in P2 decreases in the presence of one molecule water. However, MP2 calculated Gibbs free energy barrier for P1 path (AW → AW-TS, 69.5 kJ mol^{-1}) is lower than P2 (BW → BW-TS, 75.6 kJ mol^{-1}). A conspicuous consistency was found between the energy barrier of B3LYP and MP2 methods as shown in Table 3.

The keto–enol tautomerization of 1,3-IM in P4 (CH2CO → CHCOH) may be also affected by presence of water. In this process, water acts as a bridge between CO and CH_2 groups. After formation of the mono-hydrated tautomers of 1,3-IM, the proton-transfer reactions may occur from CH_2 to CO to form enol tautomer. The geometric parameters of the dimers and transition states for the CW → CW-TS in this path are given in

Figure 2. In comparison to direct proton transfer, the presence of a water molecule reduces the energy barrier by 136.2 kJ mol^{-1} in P4. Thus, keto–enol tautomerization in P4 is even facilitated by inclusion of H_2O. The higher energy barrier for CW → CW-TS with respect to A(B)W → A(B)W-TS can be attributed to the big deformation of the structure of monomer in CW → CW-TS. At both MP2 and B3LYP levels, the presence of water facilitates the proton transfer in all paths.

From Table 4, charge-transfer energy associated with $lp_S \rightarrow \sigma^*_{C2-N3}$ interaction decreases upon complex formation of AW. These interactions in AW-TS are stronger than the corresponding interactions in AW complexes. In AW dimer, lp(S) → σ^*(O13–H12) and lp(O13) → σ^*(N3–H7) intermolecular interactions are replaced by lp(O13) → σ^*(S–H12) and lp(N3) → σ^*(O13–H7) interactions in AW-TSs which are stronger than those observed in ground states.

A comparison of the natural charge of atoms in free 1,3-IM with AW and BW complexes in Table 4 shows that the charge transfer in complexes occurs from W to 1,3-IM by 0.0061e and 0.0003e, respectively. As it can be seen in Table 4, complex formation of AW results in an increase of the electronic charge of S and C2 atoms. Both C2 and S atoms lose electronic charge on going from AW to AW-TS, whereas C4 and O8 atoms gain electronic charge on going from BW to BW-TS. Our results show that the H7 atom in AW and BW complexes loses electronic charge upon TS formation by 0.0372 and 0.0264e, respectively. Besides, O13 atom loses electronic charge in A(B)W to A(B)W-TS.

In comparison with direct proton transfer, the change of H7 electronic charge upon TS formation in water-assisted mechanism is smaller than in the direct case. The value for 1,3-IM to TS1, 1,3-IM to TS2, AW to AW-TS and BW to BW-TS processes is 0.1565, 0.3203, 0.0372, and 0.0264e, respectively. Thus, it is expected that the energy barrier in the presence of water decreases, as calculated.

Conclusion

The direct and water-assisted proton transfer in 2-thioxoimidazolidin-4-one, via two keto/enol and thione/thiol mechanisms was investigated by using DFT (B3LYP) and ab initio (MP2) methods in gas phase. A conspicuous consistency was found between the results of B3LYP and MP2 calculations. The calculations at both levels show that 1,3-IM is more stable than other isomers. Because direct proton transfer takes place through a four-member ring transition structure, both thione and keto forms cannot easily transfer the proton from the N to S or O. Nevertheless, the energy barrier for tautomerism of thione/thiol (P1 and P3 paths) is smaller than keto/enol (P2 and P4 paths) processes. The change in structural parameters in P2 and P4 paths is greater than other paths which are in agreement with the greater energy barrier for P2 and P4 with respect to the P1 and P3 paths. The energy barrier for water-assisted proton-transfer reactions is significantly lower than direct tautomerization. The delocalization energies and natural charges were estimated by NBO analysis. The change of H7 charge upon TS formation in the water-assisted mechanism is smaller than in the direct path. It may be explained that the small change in atomic charge of H7 in the water-assisted mechanism causes the decrease in the energy barrier.

References

1 D. S. Ahn, S. Lee, B. Kim, *Chem. Phys. Lett.* **2004**, *390*, 384.

2 S.-W. Park, D.-S. Ahn, S. Lee, *Chem. Phys. Lett.* **2003**, *371*, 74.

3 D.-S. Ahn, S.-W. Park, I.-S. Jeon, M.-K. Lee, N.-H. Kim, Y.-H. Han, S. Lee, *J. Phys. Chem. B* **2003**, *107*, 14109.

4 S. Alavi, D. L. Thompson, *J. Chem. Phys.* **2002**, *117*, 2599.

5 F. Madeja, M. Havenith, *J. Chem. Phys.* **2002**, *117*, 7162.

6 J. Carlsson, H. Drevin, R. Axén, *J. Biochem.* **1978**, *173*, 723.

7 A. Arnoldi, S. Drasso, G. Meinardi, L. Merlini, *Eur. J. Med. Chem.* **1988**, *23*, 149.

8 H. Preut, F. Huber, K.-H. Hengstmann, *Acta Crystallogr., Sect. C* **1988**, *44*, 468.

9 P. Mura, S. D. Robinson, *Acta Crystallogr., Sect. C* **1984**, *40*, 1798.

10 A. R. Katritzky, K. Jug, D. C. Oniciu, *Chem. Rev.* **2001**, *101*, 1421.

11 S. Stoyanov, T. Stoyanova, P. D. Akrivos, P. Karagiannidis, P. Nikolov, *J. Heterocycl. Chem.* **1996**, *33*, 927.

12 J. S. Kwiatkowski, J. L. Leszczynski, *THEOCHEM* **1996**, *376*, 325.

13 A. Ladjarafi, H. Meghezzi, A. Boucekkine, *THEOCHEM* **2004**, *709*, 129.

14 D. Moran, K. Sukcharoenphon, R. Puchta, H. F. Schaefer, III, P. R. Schleyer, C. D. Hoff, *J. Org. Chem.* **2002**, *67*, 9061.

15 A. Fu, H. Li, D. Du, *THEOCHEM* **2006**, *767*, 51.

16 V. Martinez-Merino, M. J. Gil, *J. Chem. Soc., Perkin Trans. 2* **1999**, 33.

17 V. Martinez-Merino, M. J. Gil, *J. Chem. Soc., Perkin Trans. 2* **1999**, 801.

18 A. Bayer, *Liebigs Ann. Chem.* **1861**, *117*, 178.

19 N. Karali, A. Gursoy, N. Terzioglu, S. Ozkirimli, H. Ozer, A. C. Ekinci, *Arch. Pharm.* **1998**, *331*, 254.

20 G. G. Muccioli, D. Martin, G. K. E. Scriba, W. Poppitz, J. H. Poupaert, J. Wouters, D. M. Lambert, *J. Med. Chem.* **2005**, *48*, 2509.

21 S. Bouzroura, L. Hammal, B. Nedjar-Kolli, F. Balegroune, M. Hamadène, S. Poulain, *Synth. Commun.* **2008**, *38*, 448.

22 C. Laurence, M. J. El Ghomari, M. Lucon, *J. Chem. Soc., Perkin Trans. 2* **1998**, 1159.

23 A. Suszka, *J. Chem. Soc., Perkin Trans. 2* **1985**, 531.

24 M. J. Frisch, G. W. Trucks, H. B. Schlegel, G. E. Scuseria, M. A. Robb, J. R. Cheeseman, V. G. Zakrzewski, J. A. Montgomery, Jr., R. E. Stratmann, J. C. Burant, S. Dapprich, J. M. Millam, A. D. Daniels, K. N. Kudin, M. C. Strain, O. Farkas, J. Tomasi, V. Barone, M. Cossi, R. Cammi, B. Mennucci, C. Pomelli, C. Adamo, S. Clifford, J. Ochterski, G. A. Petersson, P. Y. Ayala, Q. Cui, K. Morokuma, D. K. Malick, A. D. Rabuck, K. Raghavachari, J. B. Foresman, J. Cioslowski, J. V. Ortiz, A. G. Baboul, B. B. Stefanov, G. Liu, A. Liashenko, P. Piskorz, I. Komaromi, R. Gomperts, R. L. Martin, D. J. Fox, T. Keith, M. A. Al-Laham, C. Y. Peng, A. Nanayakkara, C. Gonzalez, M. Challacombe, P. M. W. Gill, B. Johnson, W. Chen, M. W. Wong, J. L. Andres, C. Gonzalez, M. Head-Gordon, E. S. Replogle, J. A. Pople, *Gaussian 98, Revision A.7*, Gaussian, Inc., Pittsburgh PA, **1998**.

25 P. R. Rablen, J. W. Lockman, W. L. Jorgensen, *J. Phys. Chem. A* **1998**, *102*, 3782.

26 A. E. Reed, L. A. Curtiss, F. Weinhold, *Chem. Rev.* **1988**, *88*, 899.

27 J. T. Fermann, S. Auerbach, *J. Chem. Phys.* **2000**, *112*, 6787.